



# HHS Public Access

Author manuscript

*Adv Ther (Weinh)*. Author manuscript; available in PMC 2019 September 20.

Published in final edited form as:

*Adv Ther (Weinh)*. 2018 July ; 1(3): . doi:10.1002/adtp.201800032.

## Decellularized Extracellular Matrix Hydrogels as a Delivery Platform for MicroRNA and Extracellular Vesicle Therapeutics

**Melissa J. Hernandez<sup>#</sup>,**

Department of Bioengineering, Sanford Consortium for Regenerative Medicine, University of California, San Diego, La Jolla, CA, 92093, USA

**Roberto Gaetani<sup>#</sup>,**

Department of Bioengineering, Sanford Consortium for Regenerative Medicine, University of California, San Diego, La Jolla, CA, 92093, USA

**Vera M. Pieters,**

Department of Bioengineering, Sanford Consortium for Regenerative Medicine, University of California, San Diego, La Jolla, CA, 92093, USA

**Nathan W. Ng,**

Department of Bioengineering, Sanford Consortium for Regenerative Medicine, University of California, San Diego, La Jolla, CA, 92093, USA

**Audrey E. Chang,**

Department of Bioengineering, Sanford Consortium for Regenerative Medicine, University of California, San Diego, La Jolla, CA, 92093, USA

**Taylor R. Martin,**

Department of Bioengineering, Sanford Consortium for Regenerative Medicine, University of California, San Diego, La Jolla, CA, 92093, USA

**Eva van Ingen,**

Department of Bioengineering, Sanford Consortium for Regenerative Medicine, University of California, San Diego, La Jolla, CA, 92093, USA

**Emma A. Mol,**

Department of Cardiology, Experimental Cardiology Laboratory, University Medical Center Utrecht, Utrecht, 3584CX, NL

**Joost P.G. Sluijter,**

Department of Cardiology, Experimental Cardiology Laboratory, UMC Utrecht Regenerative Medicine Center, University Medical Center Utrecht, Utrecht, 3584CX, NL

**Karen L. Christman**

Department of Bioengineering, Sanford Consortium for Regenerative Medicine, University of California, San Diego, La Jolla, CA, 92093, USA

---

christman@eng.ucsd.edu.

<sup>#</sup>M.J.H. and R.G. contributed equally to this work.

Conflict of Interest

K.L.C. is co-founder, consultant, board member, and holds equity interest in Ventrix, Inc.

## Abstract

In the last decade, the use of microRNA (miRNA) and extracellular vesicle (EV) therapies has emerged as an alternative approach to mitigate the negative effects of several disease pathologies ranging from cancer to tissue and organ regeneration; however, delivery approaches towards target tissues have not been optimized. To alleviate these challenges, including rapid diffusion upon injection and susceptibility to degradation, porcine-derived decellularized extracellular matrix (ECM) hydrogels are examined as a potential delivery platform for miRNA and EV therapeutics. The incorporation of EVs and miRNA antagonists, including anti-miR and antago-miR, in ECM hydrogels results in a prolonged release as compared to the biologic agents alone. In addition, individual *in vitro* assessments confirm the bioactivity of the therapeutics upon release from the ECM hydrogels. This work demonstrates the feasibility of encapsulating miRNA and EV therapeutics in ECM hydrogels to enhance delivery and potentially efficacy in later *in vivo* applications.

## Keywords

microRNAs; extracellular vesicles; extracellular matrix; hydrogels

---

## 1. Introduction

Therapeutics, particularly growth factor- and cell-based, have been extensively investigated for many clinical applications including, but not limited to, cardiovascular disease,<sup>[1, 2]</sup> cancer,<sup>[3, 4]</sup> and autoimmune diseases.<sup>[5, 6]</sup> With mechanisms regulating essential biological processes such as neovascularization, extracellular matrix (ECM) remodeling, and inflammation, many growth factor- and cell-based therapies have been pursued in clinical trials, but translation to the clinic has been largely unsuccessful.<sup>[7-9]</sup> Along with a lack of demonstrated efficacy in patients, manufacturing difficulties, like shortened shelf life and high production costs, hinder the feasibility of utilizing cell and growth factor-based approaches. Although engineered growth factors have recently been introduced to overcome many of these obstacles from growth factor therapeutics,<sup>[10, 11]</sup> researchers have been exploring alternative biologics, including microRNAs (miRNAs) and extracellular vesicles (EVs).

MiRNAs, short 20-22 base pair oligonucleotides, have emerged as a promising therapeutic for many applications, including cardiovascular disease,<sup>[12]</sup> inflammatory disease,<sup>[13]</sup> metabolic disease,<sup>[14]</sup> and cancer.<sup>[15, 16]</sup> These therapies harness the ability of miRNAs to regulate post-transcriptional gene expression, which occurs via complementary binding with a target messenger RNA. Chemical modifications have been implemented to produce miRNA mimics and inhibitors with increased stability and more favorable pharmacokinetics,<sup>[18, 19]</sup> which have contributed to multiple miRNA therapeutics progressing to clinical trials.<sup>[20]</sup>

Another class of biologic products that is emerging as a potent cellular mediator in numerous physiological and pathological processes are EVs. EVs, cell-derived vesicles comprising exosomes and microvesicles, have been shown to play a major role in cell to cell

communication, allowing cells to exchange proteins, lipids and genetic materials, including mRNAs and non-coding RNAs such as miRNAs, thus making them effective regulators of tissue homeostasis and repair.<sup>[21, 22]</sup> EVs have been shown to play a major role in many physiological and pathological processes including cell signaling,<sup>[23, 24]</sup> immunity,<sup>[5, 25]</sup> cancer development and progression,<sup>[26, 27]</sup> protein clearance,<sup>[28]</sup> and infection.<sup>[29, 30]</sup> Due to their broad repertoire of bioactive molecules and biological functions,<sup>[22, 31]</sup> EVs have been investigated in many therapeutic applications including organ regeneration,<sup>[31-33]</sup> cancer,<sup>[34, 35]</sup> immune-based diseases,<sup>[36, 37]</sup> and neurodegenerative diseases.<sup>[38]</sup>

Although miRNA and EV therapeutics have resulted in significant therapeutic outcomes in many pre-clinical studies,<sup>[20, 39]</sup> these benefits are hindered by poor delivery strategies and rapid clearance soon after administration. Intravenous delivery is the main delivery route employed by these therapies, and direct injections have also been utilized; however, both of these approaches fail to capitalize on the full therapeutic potential of miRNAs and EVs. Current delivery methods, which often require large payloads, could yield undesired side effects from unspecific binding of miRNAs. In addition, degradation by endogenous nucleases and rapid diffusion represent significant obstacles.<sup>[12]</sup> Consequently, improved delivery strategies are greatly needed.

Several groups have begun exploring the use of hydrogels as a delivery platform for miRNA and EV therapies,<sup>[40, 41]</sup> but natural materials alone (i.e. without the addition of chemical crosslinkers or modifications) have not been investigated. Unlike most synthetic materials, natural materials can better mimic the *in vivo* environment, but, in particular, decellularized extracellular matrix (ECM), one type of naturally derived biomaterial, successfully maintains biochemical cues of the native tissue microenvironment. Decellularized ECM has several beneficial properties, which include promoting cellular influx,<sup>[42]</sup> and its degradation products are angiogenic,<sup>[43]</sup> chemoattractant,<sup>[43, 44]</sup> and promote cell migration and proliferation.<sup>[45]</sup> In addition, previous studies in a myocardial infarction model have confirmed the benefits of using cardiac-derived ECM hydrogels as a delivery platform for growth factors with increased arteriogenesis compared to growth factor alone and ECM hydrogel alone controls.<sup>[11, 46]</sup> These ECM hydrogels have also been used for cell delivery in a hindlimb ischemia model of peripheral artery disease, which increased cell engraftment and survival, stimulated neovascularization and could also potentially be used for cell transplantation into the myocardium.<sup>[47, 48]</sup> Along with the efficacy of these decellularized materials, the hydrogels can be delivered minimally invasively, as has been shown via catheter in the heart or a direct injection for the skeletal muscle.<sup>[47, 49, 50]</sup> With a complex mixture of proteins, we anticipated that an ample supply of binding sites would be present to facilitate the binding of nucleic acids and EVs. Additionally, ECM hydrogels could ensure localization of both miRNAs and EVs, and the nanoscale and microscale architecture of these hydrogels could promote a slow release of the payload.

Here we evaluated the use of porcine-derived decellularized ECM hydrogels as a platform for the delivery of model miRNAs and EVs (Figure 1). We performed assessments of our ECM hydrogels to provide a slow release profile and maintain bioactivity of miRNA and EV therapeutics, demonstrating that these biomaterials could be a potential delivery platform for such newer generation biologics.

## 2. Results and Discussion

Due to the earlier success with delivering growth factors and cells with tissue-derived hydrogels,<sup>[11, 46-48]</sup> we hypothesized that the ECM hydrogels would also provide an enhanced delivery platform for model miRNAs and EVs. Specifically, we expected the ECM hydrogels would prolong the release of miRNAs and EVs but would not affect the bioactivity of either therapeutic. To first evaluate retention, model miRNAs and EVs were mixed with three different types of decellularized ECM hydrogels. Specifically, myocardial, skeletal muscle, and lung ECM hydrogels were used due to differences in the composition of ECM proteins<sup>[49, 51]</sup> and to demonstrate potential broad applications of this delivery platform. Cardiac progenitor cell (CPC)-derived EVs<sup>[52]</sup> and miRNA antagonists for miR-214<sup>[53]</sup>, an anti-miR and antago-miR, were used as model therapeutics for these studies since they have been evaluated considerably and showed promising results in many therapeutic applications.<sup>[32, 54, 55]</sup>

### 2.1. MicroRNAs

For model miRNAs therapeutics, an anti-miR and antago-miR against miR-214 were used and have been shown to recover neovascularization through the regulation of angiogenic factors.<sup>[53]</sup> The release profiles from the three ECM hydrogels were evaluated for the miRNA inhibitors up to 15 days (Figure 2). Comparing the anti-miR and antago-miR, the release profiles varied significantly, likely due to hydrophobic interactions caused by the presence of a cholesterol group on the 3' end of the antago-miR. In fact, over 50% of the anti-miR was released from the ECM hydrogels by day 2 (Figure 2A), but the antago-miR did not reach 50% until around day 10 (Figure 2B). Moreover, the anti-miR was virtually completely released by day 10, but the antago-miR was not fully released until the additions of first collagenase to degrade the collagen in the ECM hydrogels and then 1.5M NaCl to dissociate residual antago-miRs. The rate of release was likely heavily facilitated by hydrophobic interactions, as indicated by the further release of antago-miR, but not anti-miR, following the addition of 1.5M NaCl. The amount of amines present in the ECM hydrogels could also contribute to modulating the release profile, since there are some differences present amongst the tissue sources. Specifically, the ECM hydrogels are all composed of a large amount of fibrillar collagen, but skeletal muscle ECM contains the most, while the myocardial and lung ECMs are similar.<sup>[49, 51]</sup> Moreover, the lung ECM consists of a large fraction of basement membrane proteins, while the myocardial ECM is composed of many matricellular proteins.

Although some release profiles did not reach 100%, it is unlikely this was due to degradation since the chemical modifications made to the miRNA inhibitors provide added stability, and RNases-free solutions were used for all experiments. For those values above 100%, this was likely due to the gels slightly breaking down towards the end of the 15 days, particularly with the antago-miR, which may have resulted in samples containing larger amounts of the miRNA inhibitors.

Since a prolonged release over a period of 1-2 weeks would likely be preferred, only the antago-miR was investigated for the *in vitro* studies. In addition, only the myocardial ECM hydrogel was studied further due to the relevance of this particular model miRNA inhibitor

in applications of cardiovascular disease, like myocardial infarction. Although the incorporation of the antago-miR into the ECM hydrogels yielded prolonged release profiles, it was necessary to assess whether the ECM hydrogels interfered with the inherent bioactivity of the encapsulated antago-miR. To evaluate the bioactivity of the released antago-miRs, supernatant collected from myocardial ECM hydrogels at days 1 and 3 was tested in a Matrigel tube formation assay with human coronary artery endothelial cells (HCAECs), since miR-214 is known to affect angiogenic-related processes (Figure 3).<sup>[53]</sup> As a control, PBS supernatant obtained from hydrogels at day 15 was used since this likely contained the maximum amount of ECM soluble factors, which could also potentially have angiogenic effects. After incubating the cells with miRNA-conditioned media for 12 hours, visual differences were observed in the degree of tube formation (Figure 3A). Compared to the PBS supernatant controls, released samples from days 1 and 3 yielded more organized tubes with significantly less cell clustering. When normalized to the PBS supernatant group, the total length increased to  $1.53 \pm 0.15$  for day 1 and  $1.42 \pm 0.08$  for day 3, and the number of junctions increased to  $1.84 \pm 0.12$  and  $1.71 \pm 0.19$  for days 1 and 3, respectively (Figure 3B). Although, the extent of tube formation did slightly decrease at day 3 relative to day 1, this was likely due to using a fixed amount of sample for each well, which contained less released antago-miR for day 3.

Overall, the use of the ECM hydrogels prolonged the release of the miRNA inhibitors, particularly the antago-miR, without impairing the bioactivity. This slower release rate would likely be favored for many therapeutic applications, and antago-miRs have been engineered to enhance efficacy *in vivo*. Specifically, the conjugation of the cholesterol group is thought to increase cellular uptake and improve *in vivo* stability.<sup>[19, 56]</sup> By combining this optimized biologic with a decellularized ECM hydrogel, the beneficial outcomes from these therapies could be further augmented.

## 2.2. Extracellular Vesicles

Similar to miRNAs, EVs have also been increasingly studied for many disease applications. In the present study, EVs derived from human cardiac progenitor cells (hCPCs)<sup>[52]</sup> were used for all experiments, as they have been shown to exert a protective effect on damaged myocardium by reducing cardiomyocytes apoptosis<sup>[55]</sup> and increasing cardiac function<sup>[57]</sup>. EVs were encapsulated into three different hydrogels and their release profile from the different scaffolds was evaluated at days 1, 3 and 7. After 7 days, approximately 40%, 45%, and 25% of EVs were released from the myocardial, skeletal, and lung ECM hydrogels, respectively. Of the released EVs, the majority were detected 1 day after encapsulation, ranging from ~ 30% in the myocardial and skeletal matrix hydrogels to ~ 20% in the lung ECM hydrogels (Figure 4A). Most of the remaining released EVs were released by day 3 and only a minimal increase was observed at day 7, indicating that a high amount of EVs were still retained in the gel. A washing step after EV labeling and before EV encapsulation was also performed to remove excess dye, thus minimizing potential artifacts from free dye. This was also indirectly confirmed by labeling the encapsulated EVs with PKH26 red fluorescent dye. The encapsulation of labeled EVs in the hydrogels conferred a pink coloration, which was still visible at the end of the release study, indicative of the presence of the encapsulated EVs (Figure 4B). We also quantified the remaining EVs by digesting the

hydrogels with collagenase, confirming that indeed the majority of EVs were still encapsulated, with some differences among the different hydrogels. In particular, the cumulative study showed that after collagenase treatment, we were able to detect ~ 80%, 70% and 45% of the encapsulated EVs in the myocardial, skeletal, and lung ECM hydrogels, respectively. Since we were not able to detect all of the encapsulated EVs, we evaluated the effects of the collagenase treatment on EV detection shortly after encapsulation. EVs were encapsulated within the different hydrogels, and, after hydrogel gelation, the gels were immediately treated with collagenase and compared with the same amount of non-encapsulated EVs. Our analysis showed that only ~ 60% of the encapsulated EVs ( $58.75 \pm 23.4\%$ ) were detected, indicating that the collagenase treatment negatively affected the EV detection, thus explaining the reason for not being able to recover all encapsulated EVs. However, we cannot exclude that some of the released EVs degraded due to experimental conditions, since it has been previously demonstrated that EVs are degraded when stored at 37°C.<sup>[58]</sup>

All ECM hydrogels provided a slow release of the encapsulated EV therapeutics; however, some differences were observed on the extent of the EV release between the different tissue sources. The level of released EVs detected in the EV-conditioned media from the lung ECM hydrogels was considerably lower than values of the myocardial ECM and the skeletal muscle ECM hydrogels. A possible explanation could be that the composition of the lung ECM hydrogels allowed for a more sustained encapsulation of the EVs compared to the muscle tissue derived ECM hydrogels. It is possible that a combination of physical entrapment, non-covalent interactions, or specific binding domains all contributed to the release profile of the encapsulated EVs. The combination of tissue-specific ECM molecules, which can affect the mechanical properties, pore size and electrostatic properties of the hydrogel could explain the differences observed among the different tissue sources.<sup>[59]</sup> Another possible mechanism behind the rate of EV release from the ECM hydrogels is the presence of matrix metalloproteinases (MMPs) in cardiac progenitor cell-derived extracellular vesicles.<sup>[60]</sup> These enzymes are generally known to induce ECM remodeling by degrading certain ECM molecules, which could modulate the degradation rate of ECM hydrogels *in vivo*.

We next evaluated if the encapsulation could negatively impact the bioactivity of the released EVs and if the released EVs would still assert their beneficial effects once released from the hydrogels. Conditioned media from EVs encapsulated in hydrogels was used to stimulate the phosphorylation of the ERK 1/2 pathway in target HCAECs and compared to the PBS supernatant collected from empty hydrogels. Western blot analysis showed that the EVs released 1 and 3 days after encapsulation significantly increased the phosphorylation of the ERK 1/2 proteins when compared to the PBS supernatant controls ( $1.54 \pm 0.07$  and  $1.21 \pm 0.04$  fold increase, respectively) (Figure 5). No differences were seen when the EV-conditioned media collected 7 days after encapsulation was used. The lack of bioactivity of the released EVs 1 week after encapsulation could likely be due to the very minimal levels released after the first days. However, the minimal observed release or lack of bioactivity of the EV-conditioned media released at day 7 could also partly be due to EV degradation in the experimental conditions, as mentioned above.

Since the EVs' therapeutic efficacy is in part mediated by exerting anti-apoptotic effects on the targeted cells,<sup>[61]</sup> we then investigated whether released EVs were also able to preserve cell survival in the presence of reactive oxygen species. Based on the pERK activation data, we only evaluated EVs released 1 and 3 days after encapsulation. A significant increase in cell survival was observed with both EV-conditioned medias when compared to the PBS supernatants (EVs:  $79.07 \pm 3.03\%$  at day 1 and  $80.08 \pm 3.06\%$  at day 3; PBS:  $71.64 \pm 3.40\%$  at day 1 and  $65.26 \pm 3.22\%$  at day 3) (Figure 6).

### 3. Conclusion and Outlook

The discovery of miRNAs and EVs as potent mediators of cellular function and tissue homeostasis has led many researchers to investigate their potential use for a wide variety of disease pathways. However, similar to cells, growth factors, or small molecules, their delivery is hampered by rapid clearance soon after administration, therefore potentially limiting their therapeutic effects. The use of decellularized ECM hydrogels has been proposed as an alternative approach to modulate the release rate of model miRNA and EV therapeutics. Our data collectively indicated that these hydrogels successfully retained the encapsulated biologics over a prolonged period of time with some differences between the therapeutics or hydrogel tissue source. Samples collected for the release profiles were also further investigated with bioactivity assays, and both the antago-miR and EVs remained bioactive after being released from the ECM hydrogel. This study demonstrates that decellularized ECM hydrogels may represent an advantageous platform for the delivery of miRNAs and EVs. Since the myocardial ECM hydrogel has already been injected via catheter in the hearts of myocardial infarction patients in a Phase I trial ([clinicaltrials.gov](https://clinicaltrials.gov) identifier), this suggests the clinical applicability of using injectable ECM hydrogels to delivery miRNAs and EVs in a wide array of disease applications.

### 4. Experimental Section

#### Extracellular matrix preparation:

Porcine-derived extracellular matrix (ECM) was prepared as previously described.<sup>[51, 62]</sup> Briefly, tissue from Yorkshire farm pigs was chopped into small cubes (2-5 mm) and decellularized with detergent for 3-5 days. Myocardial ECM, skeletal muscle ECM, and lung ECM was derived from the left ventricular myocardium, psoas muscle, and lung, respectively. For both the myocardial and skeletal muscle ECM hydrogels, decellularization was accomplished using 1% sodium dodecyl sulfate, while lung ECM hydrogels were decellularized with 0.1% sodium dodecyl sulfate. Skeletal muscle ECM hydrogels also required an additional isopropyl alcohol step to remove remaining lipids. Following decellularization, the tissue was then lyophilized and milled into a fine powder for long-term storage. Prior to use, the milled powder was partially digested with pepsin (Sigma-Aldrich) at a concentration of 10 mg ECM/1 ml pepsin solution (1 mg pepsin per 1 ml 0.1M HCl) for at least 48 hours and then neutralized to physiological pH and salt conditions. Finally, the concentration of the ECM hydrogel was adjusted to 6 mg/ml with 1X phosphate buffered saline (PBS) and then lyophilized once again for storage at  $-80^{\circ}\text{C}$ .

**Cell Culture:**

All cell lines were preserved in a humidified incubator at 37°C, 5% CO<sub>2</sub> and atmospheric O<sub>2</sub>. Human cardiac progenitor cells (hCPCs)<sup>[60]</sup> and human coronary artery endothelial cells (HCAECs) were used between passages 17-23 and 7-14, respectively. hCPCs were cultured as previously described.<sup>[63]</sup> Briefly, cells were cultured in 0.1% porcine gelatin (Sigma-Aldrich) coated flasks in growth media consisting of 10% fetal bovine serum (Thermo Fisher Scientific), 22% EBM2 (Lonza) complemented with EGM2 single quotes (Lonza) in Medium 199 (Corning), 1X non-essential amino acids (Lonza), and 1X penicillin-streptomycin (Life Technologies). HCAECs were grown in MesoEndo cell growth media (Cell Applications).

**MiRNA Preparation:**

Anti-miR and antago-miR oligonucleotides were synthesized with the following sequence: 5' – ACU GCC UGU CUG UGC CUG CUG T – 3' (Eurofins Genomics). Both oligonucleotides were designed with 2' O-methylation, 4 PTO-linkages on the 3' end, and 2 PTO-linkages on the 5' end. The antago-miR was further modified with a 3' cholesterol group. For release experiments requiring miRNA detection via fluorescence measurements, a Cy3 dye molecule was conjugated to the 5' end. All lyophilized anti-miR or antago-miR aliquots were resuspended with RNase-free water (Life Technologies) to a final concentration of 100 µM.

**Anti-miR and Antago-miR Release:**

Decellularized ECM hydrogels were prepared by resuspending lyophilized aliquots to a final concentration of 6 mg/ml with RNase-free water or a mixture of RNase-free water and miRNA inhibitors. Four micrograms of the Cy3-labeled anti-miR (n=3/ECM type) or antago-miR (n=3/ECM type) were mixed into the ECM hydrogels.<sup>[53]</sup> Hydrogels (200 µL total) were formed in microcentrifuge tubes by incubating at 37°C overnight. Larger volume gels were used for the anti-miR and antago-miR release compared to the EVs release, since concentrated amounts of the antago-miR did affect gelation *in vitro*. All ECM hydrogels were initially rinsed with 250 µL of RNase-free 1X PBS (Alfa Aesar) to remove any unincorporated anti-miR or antago-miR. After, 250 µL of RNase-free 1X PBS were added to each gel, all gels were incubated at 37°C on a shaker plate. Every 24 ± 2 hours for 15 days, 200 µL of the PBS supernatant was collected for quantification of miRNA release. On day 15 following collection of the PBS supernatant, 200 µL of bacterial collagenase (Worthington Biomedical Corporation) at 100 U/mL in a 0.1 M Tris-base, 0.25 M CaCl<sub>2</sub> solution, pH 7.4 was added to the gels to degrade the hydrogels. For complete degradation, gels were incubated at 37°C for 4 hours. Then, 200 µL of the collagenase samples were collected, and 200 µL of a 1.5 M NaCl solution was added to dissociate residual electrostatic interactions between the miRNAs and ECM hydrogels. Gels were allowed to incubate at 37°C for 1 hour prior to sample collection. The miRNA content in each of the release samples was quantified using a BioTek Synergy™ 4 Multi-Mode Microplate Reader. The Cy3 dye molecules were detected using an emission spectrum with a constant excitation at 547 nm and an emission ranging from 577 nm to 597 nm. Known amounts of the Cy3-labeled anti-miR or antago-miR were mixed with supernatant from empty ECM hydrogels to



construct individual standard curves. These standard curves were then used to determine the amount of released miRNAs. Release samples were stored at  $-80^{\circ}\text{C}$  for later analysis. To analyze the results, the amount of miRNA rinsed away on day 0 was subtracted from the original  $4\ \mu\text{g}$  and used as the total amount for calculating the cumulative percent released.

#### **Antago-miR Bioactivity – Tube Formation Assay:**

Growth-factor reduced Matrigel™ (10  $\mu\text{L}$ , Corning) was carefully pipetted into individual wells in a  $\mu$ -slide angiogenesis (Ibidi) and allowed to gel at  $37^{\circ}\text{C}$  for approximately 45 minutes. In the meantime, HCAECs were collected, and the mixture was then concentrated to 400,000 cells/mL in MesoEndo growth media for a total amount of 10,000 cells per well. In separate microcentrifuge tubes, samples were prepared to yield 50  $\mu\text{L}$  total per well. Each sample tube contained 25  $\mu\text{L}$  of sample and 25  $\mu\text{L}$  of cells in media. The sample volume was taken directly from tubes containing the collected release from days 1 and 3 and the PBS supernatant at day 15 prior to collagenase and 1.5M NaCl treatments. The experiment was done in triplicate, and data was analyzed using the Matlab AngioQuant toolbox.

#### **EV Isolation:**

hCPCs from 3 different donors were used for EV isolation. CPCs were cultured in EV-free growth media until 80% confluency was reached and the media was collected for EV isolation. To prepare EV-free growth media, 33% FBS in Medium 199 was centrifuged at 100,000 g for 16 hours at  $4^{\circ}\text{C}$  (Optima L-80 XP Ultracentrifuge) and sterile filtered. The supernatant was used to prepare growth media as described above. hCPC-conditioned media was collected and centrifuged at 2000 g for 15 minutes at  $4^{\circ}\text{C}$  (Eppendorf Centrifuge 5810R) to pellet dead cells and debris. The supernatant was then centrifuged at 10,000 g for 30 minutes at  $4^{\circ}\text{C}$  to pellet larger vesicles. The EV pellet was obtained in the last centrifuge step at 100,000 g at  $4^{\circ}\text{C}$  for 60 minutes, sterile filtered, resuspended in PBS and stored at  $4^{\circ}\text{C}$  when used the next day or at  $-80^{\circ}\text{C}$  for long-term storage. EV concentration was measured using the Micro BCA Protein Assay Kit (Thermo Scientific). Bovine serum albumin (BSA) standards were prepared within the range of 0.5  $\mu\text{g}/\text{ml}$  to 200  $\mu\text{g}/\text{ml}$ . Both standards and EV samples were incubated with Micro BCA Working Reagent at  $37^{\circ}\text{C}$  for 2 hours and analyzed with a BioTek Synergy™ 4 Multi-Mode Microplate Reader at 562 nm. EV concentration was determined by comparing the values of the EV samples with the known concentrations of the standards.

#### **EV Labeling:**

EVs were fluorescently labeled with  $2 \times 10^{-6}$  M PKH26 red fluorescent dye (Sigma; PKH26 Red Fluorescent cell linker mini-kit for general cell membrane labeling, MINI26-1KT) according to the manufacturer's protocol. The labeling reaction was stopped by adding 3 mL of 33% EV-free FBS in M199 and ultracentrifuged as previously described. After centrifugation, the pellet was resuspended in PBS at a concentration of 0.5  $\mu\text{g}/\mu\text{l}$  and used for encapsulation experiments.

**EV Detection:**

EV release from decellularized ECM hydrogels was measured using an EV capture method with antibody-coated magnetic beads. Samples were incubated with anti-CD63-coated magnetic beads (ExoCap, JSR Life Sciences) overnight and washed by aspiration on the magnet and adding 2% BSA in PBS (washing buffer). Secondary CD63-Alexa647 antibody in PBS (BD Bioscience) was added and incubated for 2 hours at room temperature while shaking. Beads were washed with washing buffer and resuspended in 0.25% BSA in PBS. Mean fluorescent intensity of the samples was measured by FACS (Canto).

**EV Bioactivity – Stimulation of pERK Expression:**

In a flat bottom 24 well plate, 100,000 HCAECs were plated in MesoEndo cell growth media. After 24 hours, the cells were starved by replacing media with Medium 199 for 3 hours. Following starvation, HCAECs were incubated with 200  $\mu$ l myocardial ECM hydrogel-conditioned PBS from gels with or without encapsulated EVs. Samples from days 1 (n=4/group), 3 (n=3/group), and 7 (n=4/group) were examined. Cells were lysed with cOmplete Lysis-M buffer (Roche) on ice for 5 minutes. Lysate was centrifuged at 14,000 g for 10 minutes at 4°C, and the supernatant was stored at -80°C. To prepare the samples for gel electrophoresis, 14.5  $\mu$ l HCAEC lysate was combined with 7.5  $\mu$ l 4X NuPAGE LDS Sample Buffer (Thermo Fisher Scientific) and 3  $\mu$ l NuPAGE Sample Reducing Agent (Thermo Fisher Scientific). The samples were then heated for 10 minutes at 70°C. A NuPAGE 4-12% Bis-Tris Protein Gel (Thermo Fisher Scientific) was loaded with 20  $\mu$ l sample and 10  $\mu$ l PageRuler Prestained Protein Ladder (Thermo Fisher Scientific). The gel was placed in the XCell SureLock Mini-Cell Electrophoresis System (Thermo Fisher Scientific), and the chambers were filled with 1X NuPAGE MOPS SDS Running Buffer (Thermo Fisher Scientific). In addition, 500  $\mu$ l of NuPAGE Antioxidant (Thermo Fisher Scientific) was added to the inner chamber. Electrophoresis was performed at 200 volts for 50 minutes. Western blot was performed using the XCell SureLock Mini-Cell Electrophoresis System filled with 1X NuPAGE Transfer Buffer (Thermo Fisher Scientific) in 10% methanol in deionized water. Proteins were transferred from the gel onto a 0.45- $\mu$ m nitrocellulose membrane (Bio-Rad Laboratories) at 35 volts for 1 hour on ice. The membrane was blocked in 5% BSA (Gemini Bio) in TBS for 1 hour at room temperature, followed by incubation with primary antibodies 1:500 phospho-p44/42 MAPK (Thr202/Tyr204) (Cell Signal) and 1:3000  $\beta$ 3 tubulin (Abcam) in 0.5% BSA in TBS for 1 hour at room temperature. The membrane was then incubated with secondary antibody 1:1000 goat anti-rabbit IgG HRP (Abcam) in 5% milk 0.1% Tween in TBS for 1 hour at room temperature. Prior to imaging, the membrane was incubated with Pierce ECL Western Blotting Substrate (Thermo Fisher Scientific) for 1 minute and imaged with the Bio-Rad ChemiDoc MP System using Image Lab 3.0 software.

**EV Bioactivity – Anti-Apoptotic Effect:**

A 96-well plate was coated with 0.1% porcine gelatin and 7500 hCPCs per well were seeded and incubated in growth media overnight. After 24 hours, the media was replaced by 10% alamarBlue Cell Viability Reagent (Invitrogen) in growth media and incubated for 4 hours at 37°C. AlamarBlue was transferred to a flat bottom 96-well plate (100  $\mu$ l per well) and

baseline values were measured in a BioTek Synergy™ 4 Multi-Mode Microplate Reader at 550 nm excitation and 585 nm emission. After baseline measurements, cells were incubated with 25 µM H<sub>2</sub>O<sub>2</sub> in myocardial ECM hydrogel-conditioned PBS from gels with or without encapsulated EVs for 16 hours at 37°C followed by incubation with 10% alamarBlue in growth media for 4 hours at 37°C. AlamarBlue was again transferred to a flat bottom 96-well plate (100 µl per well), and the final values were measured with the microplate reader. Cell survival was measured as % of viable cells compared to baseline measurements. Six and seven replicates were performed for day 1 and day 3 samples, respectively.

### Statistical Analysis:

Results are displayed as mean ± standard error of the mean. GraphPad Prism 6 was used for statistical analyses. For comparisons between the miRNA release samples and PBS supernatant control, a one-way ANOVA with a Dunnett's post hoc test was used. EV release samples and the PBS supernatant controls were compared with a Student's t-test. Significance was accepted at  $p < 0.05$ .

### Supplementary Material

Refer to Web version on PubMed Central for supplementary material.

### Acknowledgements

M.J.H. and R.G. contributed equally to this work. This work was supported by the NIH NHLBI (R01HL113468). M.J.H. was supported by the NHLBI (1F31HL132584, T32HL105373). J.P.G.S. and E.M. are supported by Horizon2020 ERC-2016-COG EVICARE (725229), the Project SMARTCARE-II of the BioMedicalMaterials institute, co-funded by the ZonMw-TAS program (#116002016), the Dutch Ministry of Economic Affairs, Agriculture and Innovation and the Netherlands CardioVascular Research Initiative (CVON): the Dutch Heart Foundation, Dutch Federations of University Medical Centers, the Netherlands Organization for Health Research and Development, and the Royal Netherlands Academy of Sciences.

### References

- [1]. Segers VF, Lee RT, Stem-cell therapy for cardiac disease, *Nature* 2008, 451, 937. [PubMed: 18288183]
- [2]. Hastings CL, Roche ET, Ruiz-Hernandez E, Schenke-Layland K, Walsh CJ, Duffy GP, Drug and cell delivery for cardiac regeneration, *Adv Drug Deliv Rev* 2015, 84, 85. [PubMed: 25172834]
- [3]. Woodburn JR, The epidermal growth factor receptor and its inhibition in cancer therapy, *Pharmacol Ther* 1999, 82, 241. [PubMed: 10454201]
- [4]. Tugues S, Koch S, Gualandi L, Li X, Claesson-Welsh L, Vascular endothelial growth factors and receptors: anti-angiogenic therapy in the treatment of cancer, *Mol Aspects Med* 2011, 32, 88. [PubMed: 21565214]
- [5]. Robbins PD, Morelli AE, Regulation of immune responses by extracellular vesicles, *Nat Rev Immunol* 2014, 14, 195. [PubMed: 24566916]
- [6]. Munir H, McGettrick HM, Mesenchymal Stem Cell Therapy for Autoimmune Disease: Risks and Rewards, *Stem Cells Dev* 2015, 24, 2091. [PubMed: 26068030]
- [7]. Trounson A, McDonald C, Stem Cell Therapies in Clinical Trials: Progress and Challenges, *Cell Stem Cell* 2015, 17, 11. [PubMed: 26140604]
- [8]. Feyen DAM, Gaetani R, Doevendans PA, Sluijter JPG, Stem cell-based therapy: Improving myocardial cell delivery, *Adv Drug Deliv Rev* 2016, 106, 104. [PubMed: 27133386]
- [9]. Sluijter JPG, Davidson SM, Boulanger CM, Buzas EI, de Kleijn DPV, Engel FB, Giricz Z, Hausenloy DJ, Kishore R, Lecour S, Leor J, Madonna R, Perrino C, Prunier F, Sahoo S,

Schiffelers RM, Schulz R, Van Laake LW, Ytrehus K, Ferdinandy P, Extracellular vesicles in diagnostics and therapy of the ischaemic heart: Position Paper from the Working Group on Cellular Biology of the Heart of the European Society of Cardiology, Cardiovascular research 2018, 114, 19. [PubMed: 29106545]

- [10]. Liu CJ, Jones DS 2nd, Tsai PC, Venkataramana A, Cochran JR, An engineered dimeric fragment of hepatocyte growth factor is a potent c-MET agonist, FEBS Lett. 2014, 588, 4831. [PubMed: 25451235]
- [11]. Sonnenberg SB, Rane AA, Liu CJ, Rao N, Agmon G, Suarez S, Wang R, Munoz A, Bajaj V, Zhang S, Braden R, Schup-Magoffin PJ, Kwan OL, DeMaria AN, Cochran JR, Christman KL, Delivery of an engineered HGF fragment in an extracellular matrix-derived hydrogel prevents negative LV remodeling post-myocardial infarction, Biomaterials 2015, 45, 56. [PubMed: 25662495]
- [12]. van Rooij E, Olson EN, MicroRNA therapeutics for cardiovascular disease: opportunities and obstacles, Nat Rev Drug Discov 2012, 11, 860. [PubMed: 23080337]
- [13]. Dai R, Ahmed SA, MicroRNA, a new paradigm for understanding immunoregulation, inflammation, and autoimmune diseases, Transl Res 2011, 157, 163. [PubMed: 21420027]
- [14]. Rottiers V, Naar AM, MicroRNAs in metabolism and metabolic disorders, Nat Rev Mol Cell Biol 2012, 13, 239. [PubMed: 22436747]
- [15]. Chen Y, Gao DY, Huang L, In vivo delivery of miRNAs for cancer therapy: challenges and strategies, Adv Drug Deliv Rev 2015, 81, 128. [PubMed: 24859533]
- [16]. Kasinski AL, Slack FJ, Epigenetics and genetics. MicroRNAs en route to the clinic: progress in validating and targeting microRNAs for cancer therapy, Nat Rev Cancer 2011, 11, 849. [PubMed: 22113163]
- [17]. Chekulaeva M, Filipowicz W, Mechanisms of miRNA-mediated post-transcriptional regulation in animal cells, Curr Opin Cell Biol 2009, 21, 452. [PubMed: 19450959]
- [18]. Lennox KA, Behlke MA, Chemical modification and design of anti-miRNA oligonucleotides, Gene Ther 2011, 18, 1111. [PubMed: 21753793]
- [19]. Krutzfeldt J, Rajewsky N, Braich R, Rajeev KG, Tuschl T, Manoharan M, Stoffel M, Silencing of microRNAs in vivo with 'antagomirs', Nature 2005, 438, 685. [PubMed: 16258535]
- [20]. van Rooij E, Purcell AL, Levin AA, Developing microRNA therapeutics, Circ Res 2012, 110, 496. [PubMed: 22302756]
- [21]. Pitt JM, Kroemer G, Zitvogel L, Extracellular vesicles: masters of intercellular communication and potential clinical interventions, J Clin Invest 2016, 126, 1139. [PubMed: 27035805]
- [22]. van Niel G, D'Angelo G, Raposo G, Shedding light on the cell biology of extracellular vesicles, Nat Rev Mol Cell Biol 2018.
- [23]. Valadi H, Ekstrom K, Bossios A, Sjostrand M, Lee JJ, Lotvall JO, Exosome-mediated transfer of mRNAs and microRNAs is a novel mechanism of genetic exchange between cells, Nat Cell Biol 2007, 9, 654. [PubMed: 17486113]
- [24]. Cossetti C, Iraci N, Mercer TR, Leonardi T, Alpi E, Drago D, Alfaro-Cervello C, Saini HK, Davis MP, Schaeffer J, Vega B, Stefanini M, Zhao C, Muller W, Garcia-Verdugo JM, Mathivanan S, Bachi A, Enright AJ, Mattick JS, Pluchino S, Extracellular vesicles from neural stem cells transfer IFN-gamma via Ifngr1 to activate Stat1 signaling in target cells, Mol Cell 2014, 56, 193. [PubMed: 25242146]
- [25]. Robbins PD, Dorrnsoro A, Booker CN, Regulation of chronic inflammatory and immune processes by extracellular vesicles, J Clin Invest 2016, 126, 1173. [PubMed: 27035808]
- [26]. Kosaka N, Yoshioka Y, Fujita Y, Ochiya T, Versatile roles of extracellular vesicles in cancer, J Clin Invest 2016, 126, 1163. [PubMed: 26974161]
- [27]. Naito Y, Yoshioka Y, Yamamoto Y, Ochiya T, How cancer cells dictate their microenvironment: present roles of extracellular vesicles, Cell Mol Life Sci 2017, 74, 697. [PubMed: 27582126]
- [28]. Yuyama K, Sun H, Mitsutake S, Igarashi Y, Sphingolipid-modulated exosome secretion promotes clearance of amyloid-beta by microglia, J. Biol. Chem. 2012, 287, 10977. [PubMed: 22303002]
- [29]. Bukong TN, Momen-Heravi F, Kodys K, Bala S, Szabo G, Exosomes from hepatitis C infected patients transmit HCV infection and contain replication competent viral RNA in complex with Ago2-miR122-HSP90, PLoS Pathog 2014, 10, e1004424. [PubMed: 25275643]

- [30]. Wiley RD, Gummuluru S, Immature dendritic cell-derived exosomes can mediate HIV-1 trans infection, *Proc Natl Acad Sci U S A* 2006, 103, 738. [PubMed: 16407131]
- [31]. S ELA, Mager I, Breakefield XO, Wood MJ, Extracellular vesicles: biology and emerging therapeutic opportunities, *Nat Rev Drug Discov* 2013, 12, 347. [PubMed: 23584393]
- [32]. Mol EA, Goumans MJ, Sluijter JPG, Cardiac Progenitor-Cell Derived Exosomes as Cell-Free Therapeutic for Cardiac Repair, *Adv Exp Med Biol* 2017, 998, 207. [PubMed: 28936742]
- [33]. Jing H, He X, Zheng J, Exosomes and regenerative medicine: state of the art and perspectives, *Transl Res* 2018.
- [34]. Tickner JA, Urquhart AJ, Stephenson SA, Richard DJ, O'Byrne KJ, Functions and therapeutic roles of exosomes in cancer, *Front Oncol* 2014, 4, 127. [PubMed: 24904836]
- [35]. Vader P, Breakefield XO, Wood MJ, Extracellular vesicles: emerging targets for cancer therapy, *Trends Mol Med* 2014, 20, 385. [PubMed: 24703619]
- [36]. Borger V, Bremer M, Ferrer-Tur R, Gockeln L, Stambouli O, Becic A, Giebel B, Mesenchymal Stem/Stromal Cell-Derived Extracellular Vesicles and Their Potential as Novel Immunomodulatory Therapeutic Agents, *Int J Mol Sci* 2017, 18.
- [37]. Tan L, Wu H, Liu Y, Zhao M, Li D, Lu Q, Recent advances of exosomes in immune modulation and autoimmune diseases, *Autoimmunity* 2016, 49, 357. [PubMed: 27259064]
- [38]. Quek C, Hill AF, The role of extracellular vesicles in neurodegenerative diseases, *Biochem. Biophys. Res. Commun.* 2017, 483, 1178. [PubMed: 27659705]
- [39]. Akyurekli C, Le Y, Richardson RB, Fergusson D, Tay J, Allan DS, A systematic review of preclinical studies on the therapeutic potential of mesenchymal stromal cell-derived microvesicles, *Stem Cell Rev* 2015, 11, 150.
- [40]. Hernandez MJ, Christman KL, Designing Acellular Injectable Biomaterial Therapeutics for Treating Myocardial Infarction and Peripheral Artery Disease, *JACC Basic Transl Sci* 2017, 2, 212. [PubMed: 29057375]
- [41]. Curtin CM, Castano IM, O'Brien FJ, Scaffold-Based microRNA Therapies in Regenerative Medicine and Cancer, *Advanced healthcare materials* 2018, 7.
- [42]. Rieder E, Nigisch A, Dekan B, Kasimir MT, Muhlbacher F, Wolner E, Simon P, Weigel G, Granulocyte-based immune response against decellularized or glutaraldehyde cross-linked vascular tissue, *Biomaterials* 2006, 27, 5634. [PubMed: 16889827]
- [43]. Li F, Li W, Johnson S, Ingram D, Yoder M, Badylak S, Low-molecular-weight peptides derived from extracellular matrix as chemoattractants for primary endothelial cells, *Endothelium* 2004, 11, 199. [PubMed: 15370297]
- [44]. Beattie AJ, Gilbert TW, Guyot JP, Yates AJ, Badylak SF, Chemoattraction of progenitor cells by remodeling extracellular matrix scaffolds, *Tissue Eng Part A* 2009, 15, 1119. [PubMed: 18837648]
- [45]. Reing JE, Zhang L, Myers-Irvin J, Cordero KE, Freytes DO, Heber-Katz E, Bedelbaeva K, McIntosh D, Dewilde A, Braunhut SJ, Badylak SF, Degradation products of extracellular matrix affect cell migration and proliferation, *Tissue Eng Part A* 2009, 15, 605. [PubMed: 18652541]
- [46]. Seif-Naraghi SB, Horn D, Schup-Magoffin PJ, Christman KL, Injectable extracellular matrix derived hydrogel provides a platform for enhanced retention and delivery of a heparin-binding growth factor, *Acta Biomaterialia* 2012, 8, 3695. [PubMed: 22750737]
- [47]. Rao N, Agmon G, Tierney MT, Ungerleider JL, Braden RL, Sacco A, Christman KL, Engineering an Injectable Muscle-Specific Microenvironment for Improved Cell Delivery Using a Nanofibrous Extracellular Matrix Hydrogel, *ACS Nano* 2017, 11, 3851. [PubMed: 28323411]
- [48]. Gaetani R, Yin C, Srikumar N, Braden R, Doevendans PA, Sluijter JP, Christman KL, Cardiac-Derived Extracellular Matrix Enhances Cardiogenic Properties of Human Cardiac Progenitor Cells, *Cell Transplant* 2016, 25, 1653. [PubMed: 26572770]
- [49]. Ungerleider JL, Johnson TD, Hernandez MJ, Elhag DI, Braden RL, Dzieciatkowska M, Osborn KG, Hansen KC, Mahmud E, Christman KL, Extracellular Matrix Hydrogel Promotes Tissue Remodeling, Arteriogenesis, and Perfusion in a Rat Hindlimb Ischemia Model, *JACC: Basic Translational Science* 2016, 1, 32. [PubMed: 27104218]
- [50]. Singelyn JM, Sundaramurthy P, Johnson TD, Schup-Magoffin PJ, Hu DP, Faulk DM, Wang J, Mayle KM, Bartels K, Salvatore M, Kinsey AM, Demaria AN, Dib N, Christman KL, Catheter-

deliverable hydrogel derived from decellularized ventricular extracellular matrix increases endogenous cardiomyocytes and preserves cardiac function post-myocardial infarction, *J Am Coll Cardiol* 2012, 59, 751. [PubMed: 22340268]

- [51]. Merna N, Fung KM, Wang JJ, King CR, Hansen KC, Christman KL, George SC, Differential beta3 Integrin Expression Regulates the Response of Human Lung and Cardiac Fibroblasts to Extracellular Matrix and Its Components, *Tissue Eng Part A* 2015, 21, 2195. [PubMed: 25926101]
- [52]. Vrijksen KR, Maring JA, Chamuleau SA, Verhage V, Mol EA, Deddens JC, Metz CH, Lodder K, van Eeuwijk EC, van Dommelen SM, Doevendans PA, Smits AM, Goumans MJ, Sluijter JP, Exosomes from Cardiomyocyte Progenitor Cells and Mesenchymal Stem Cells Stimulate Angiogenesis Via EMMPRIN, *Advanced healthcare materials* 2016, 5, 2555. [PubMed: 27570124]
- [53]. van Mil A, Grundmann S, Goumans MJ, Lei Z, Oerlemans MI, Jaksani S, Doevendans PA, Sluijter JP, MicroRNA-214 inhibits angiogenesis by targeting Quaking and reducing angiogenic growth factor release, *Cardiovascular research* 2012, 93, 655. [PubMed: 22227154]
- [54]. Aurora AB, Mahmoud AI, Luo X, Johnson BA, van Rooij E, Matsuzaki S, Humphries KM, Hill JA, Bassel-Duby R, Sadek HA, Olson EN, MicroRNA-214 protects the mouse heart from ischemic injury by controlling Ca(2)(+) overload and cell death, *J Clin Invest* 2012, 122, 1222. [PubMed: 22426211]
- [55]. Chen L, Wang Y, Pan Y, Zhang L, Shen C, Qin G, Ashraf M, Weintraub N, Ma G, Tang Y, Cardiac progenitor-derived exosomes protect ischemic myocardium from acute ischemia/reperfusion injury, *Biochem. Biophys. Res. Commun.* 2013, 431, 566. [PubMed: 23318173]
- [56]. Krutzfeldt J, Kuwajima S, Braich R, Rajeev KG, Pena J, Tuschl T, Manoharan M, Stoffel M, Specificity, duplex degradation and subcellular localization of antago-miRs, *Nucleic Acids Res.* 2007, 35, 2885. [PubMed: 17439965]
- [57]. Barile L, Lionetti V, Cervio E, Matteucci M, Gherghiceanu M, Popescu LM, Torre T, Siclari F, Moccetti T, Vassalli G, Extracellular vesicles from human cardiac progenitor cells inhibit cardiomyocyte apoptosis and improve cardiac function after myocardial infarction, *Cardiovascular research* 2014, 103, 530. [PubMed: 25016614]
- [58]. Sokolova V, Ludwig AK, Hornung S, Rotan O, Horn PA, Epple M, Giebel B, Characterisation of exosomes derived from human cells by nanoparticle tracking analysis and scanning electron microscopy, *Colloids Surf B Biointerfaces* 2011, 87, 146. [PubMed: 21640565]
- [59]. Johnson TD, Lin SY, Christman KL, Tailoring material properties of a nanofibrous extracellular matrix derived hydrogel, *Nanotechnology* 2011, 22, 494015. [PubMed: 22101810]
- [60]. Vrijksen KR, Sluijter JP, Schuchardt MW, van Balkom BW, Noort WA, Chamuleau SA, Doevendans PA, Cardiomyocyte progenitor cell-derived exosomes stimulate migration of endothelial cells, *J Cell Mol Med* 2010, 14, 1064. [PubMed: 20465578]
- [61]. Arslan F, Lai RC, Smeets MB, Akeroyd L, Choo A, Aguor EN, Timmers L, van Rijen HV, Doevendans PA, Pasterkamp G, Lim SK, de Kleijn DP, Mesenchymal stem cell-derived exosomes increase ATP levels, decrease oxidative stress and activate PI3K/Akt pathway to enhance myocardial viability and prevent adverse remodeling after myocardial ischemia/reperfusion injury, *Stem Cell Res* 2013, 10, 301. [PubMed: 23399448]
- [62]. Ungerleider JL, Johnson TD, Rao N, Christman KL, Fabrication and characterization of injectable hydrogels derived from decellularized skeletal and cardiac muscle, *Methods* 2015, 84, 53. [PubMed: 25843605]
- [63]. Smits AM, van Vliet P, Metz CH, Korfage T, Sluijter JP, Doevendans PA, Goumans MJ, Human cardiomyocyte progenitor cells differentiate into functional mature cardiomyocytes: an in vitro model for studying human cardiac physiology and pathophysiology, *Nat Protoc* 2009, 4, 232. [PubMed: 19197267]

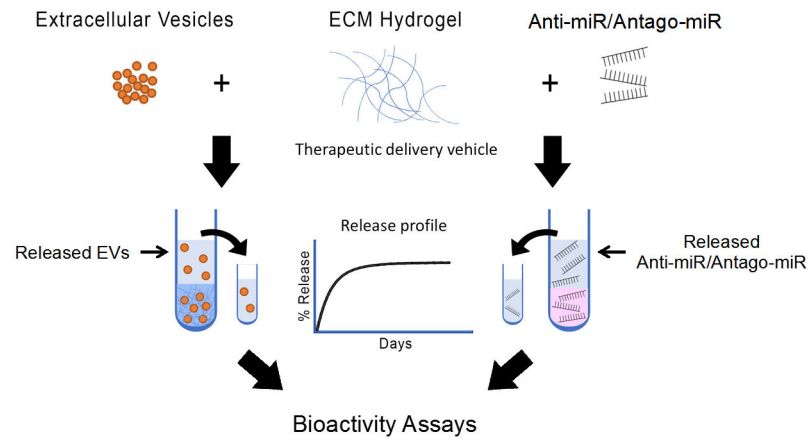


**Figure 1.** Schematic of the workflow for assessing decellularized ECM hydrogels as a delivery platform for miRNA and EV therapeutics. Anti-miRs, antago-miRs, and EVs were encapsulated in ECM hydrogels, and the release profiles were first generated. Antago-miR and EV release samples were then further analyzed to ensure the biologics remained bioactive.

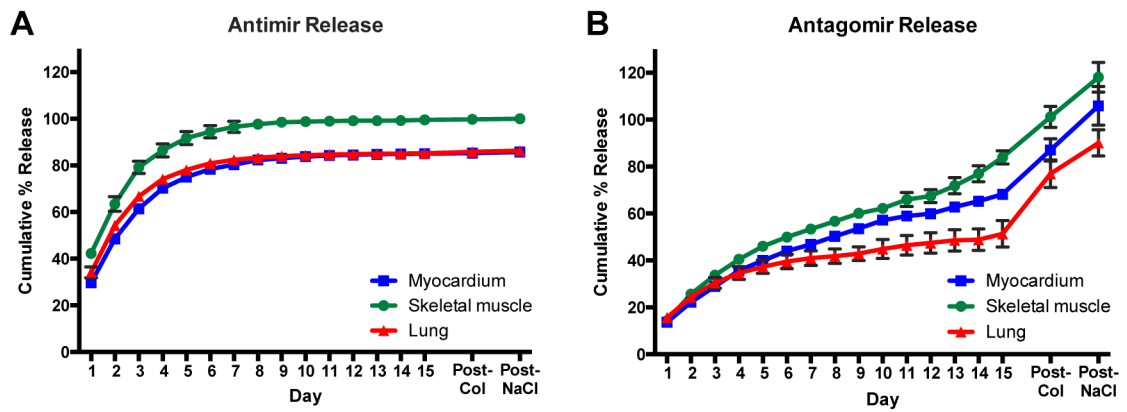


**Figure 2.**

Release profiles for miRNA inhibitors of miR-214, an anti-miR and antago-miR. Values were obtained from fluorescence measurements using the Cy3 dye molecule conjugated to each miRNA, and values exceeding 100% likely resulted from errors due to the linear fit of the generated standard curves. The anti-miR (A) yielded a more rapid release rate, likely due to the absence of a cholesterol group, which is present on the antago-miR (B). The cholesterol group introduces hydrophobic interactions, which appear to affect the release rate. Some of the error bars are too small to be visualized at each time point. n = 3/gel type



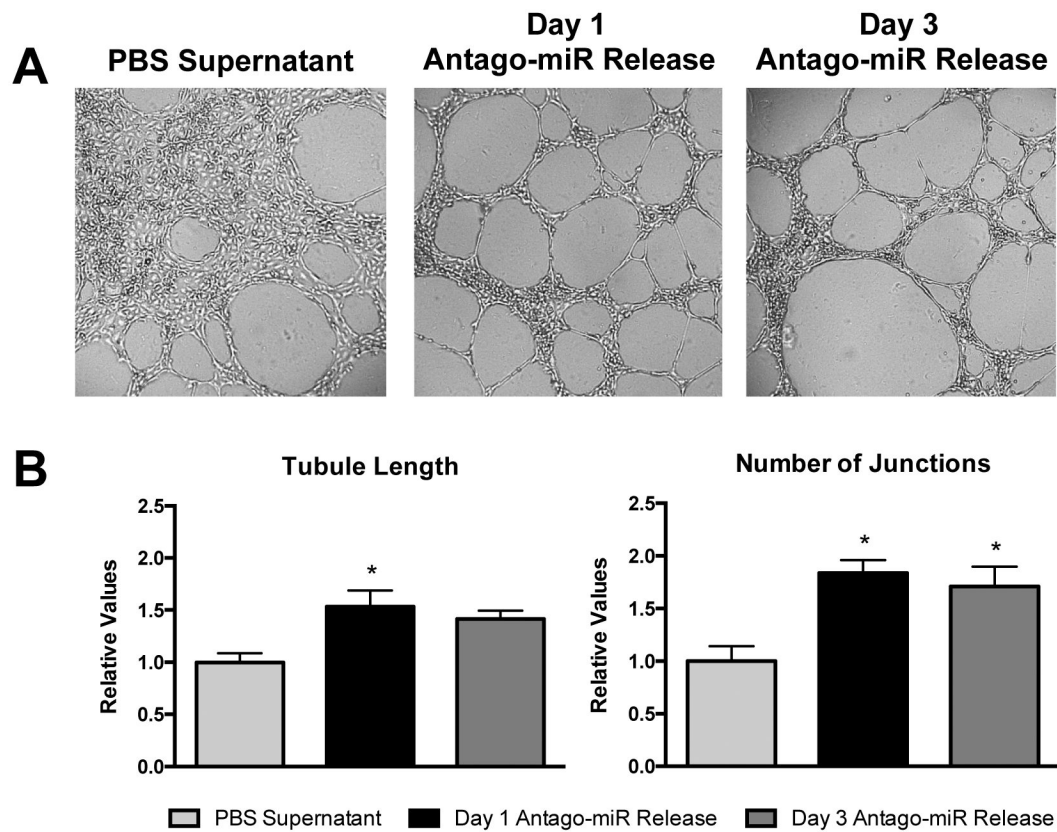


**Figure 3.**

Bioactivity of released antago-miRs in a Matrigel tube formation assay. (A) Representative images are shown for the tube formation of HCAECs on Matrigel. Since ECM soluble factors are present in the PBS supernatant group, some tube formation is seen but with a large degree of cell clustering. However, released samples from days 1 and 3 produce more organized tubes that yield relative increases in (B) tubule length and the number of junctions over the PBS control ( $n = 3/\text{group}$ ). \* $p < 0.05$  compared to the PBS supernatant control using a one-way ANOVA with a Dunnett's post hoc test.

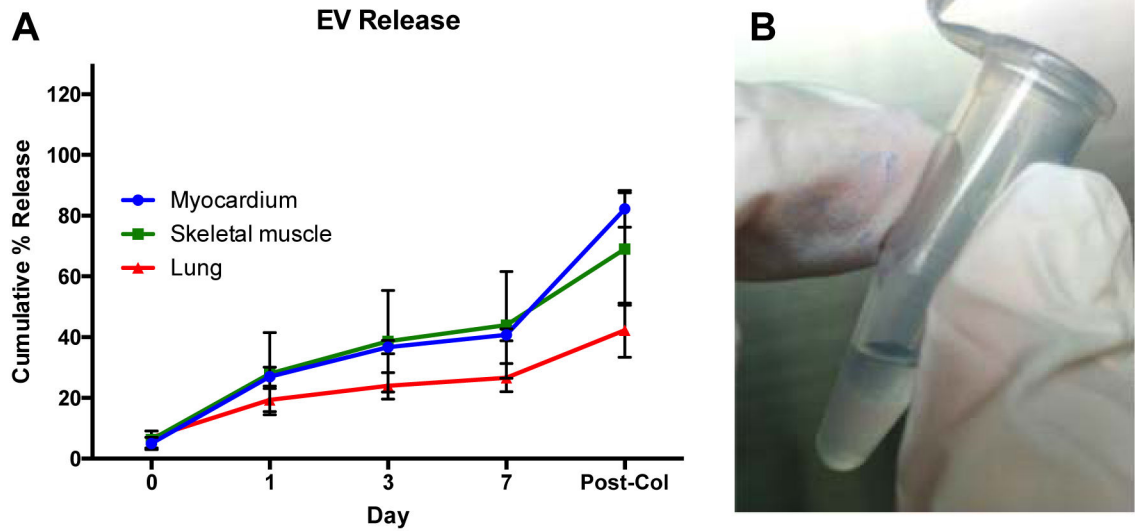


**Figure 4.** Cumulative release of hCPC-derived EVs from porcine ECM hydrogels. (A) Conditioned PBS was collected at days 0, 1, 3 and 7, and the concentration of detected EVs is shown as a percentage of the mean fluorescent intensity of 4  $\mu$ g untreated EVs. Fluorescent intensities were determined with magnetic bead capture flow cytometry. Myocardial ECM hydrogels (n = 4), skeletal muscle ECM hydrogels (n = 3), and lung ECM hydrogels (n = 3) were examined. (B) PKH26 labeled EVs confer a pink color to the gels, which is still visible after 7 days and indicates the presence of the encapsulated EVs.

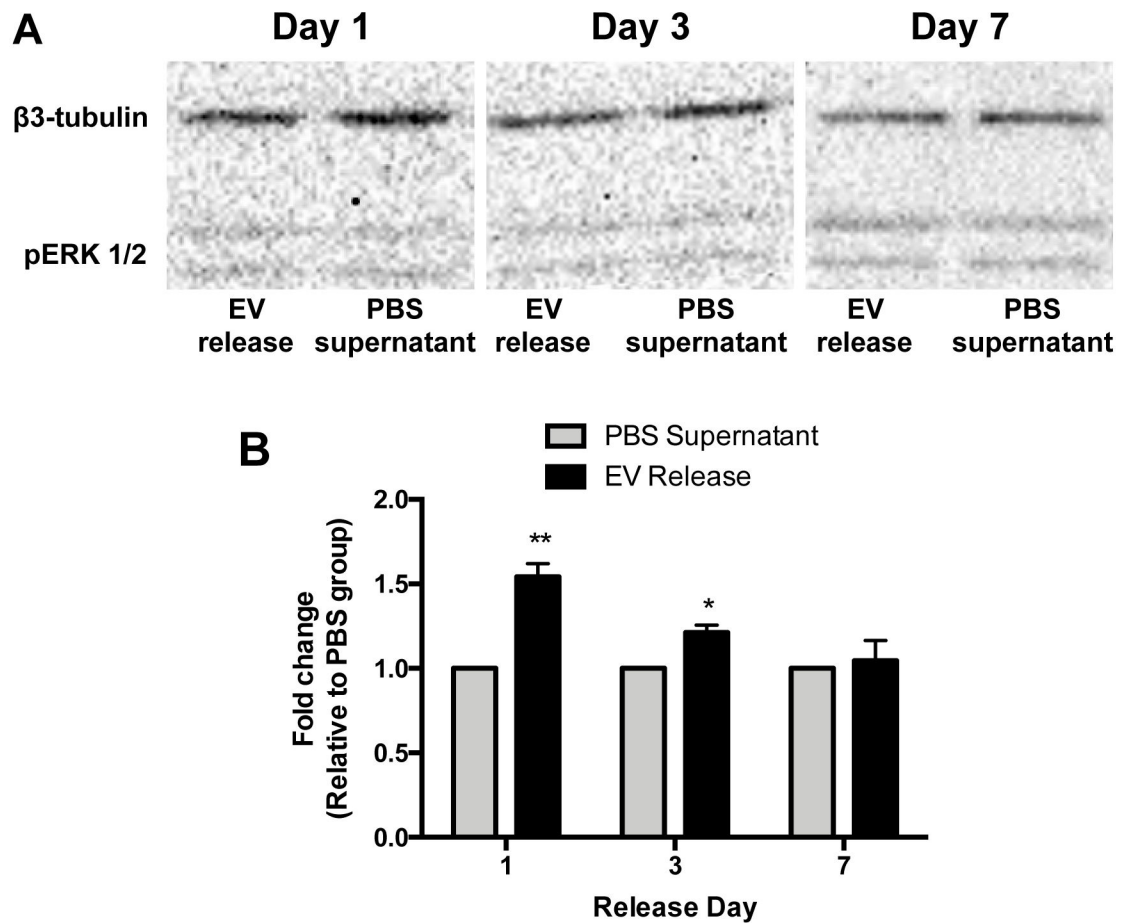


**Figure 5.**

The effect of CPC-derived EVs released from cardiac ECM hydrogels on pERK 1/2 levels in HCAECs. Cells were incubated with conditioned PBS collected at days 1 (n = 4/group), 3 (n = 3/group), and 7 (n = 4/group). The expression of pERK 1/2 was determined with western blot analysis, normalized to  $\beta$ 3-tubulin and relative to conditioned PBS from empty ECM hydrogels. \*p < 0.05 and \*\*p < 0.01 compared to PBS supernatant using a Student's t-test.

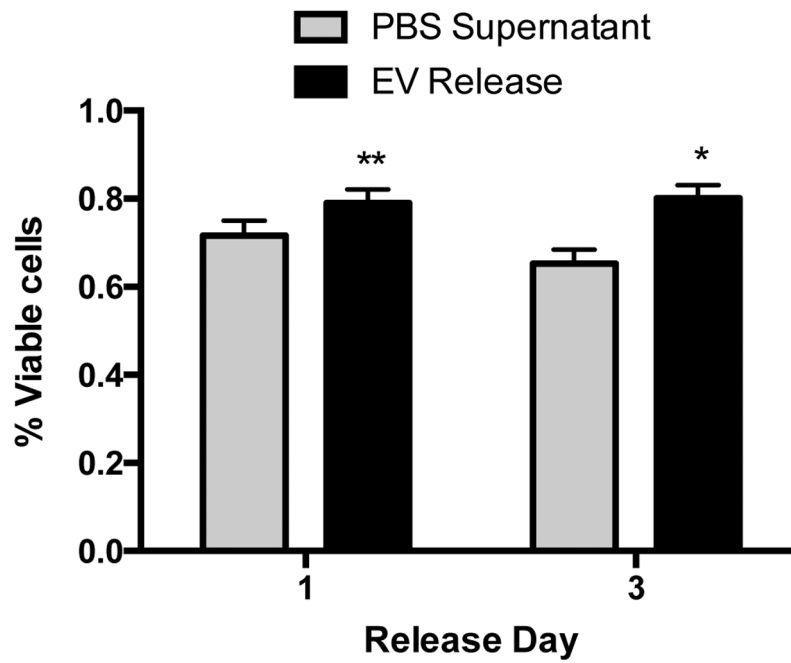


**Figure 6.**

The protective effect of CPC-derived EVs released from cardiac ECM hydrogels on  $H_2O_2$ -induced apoptosis of hCPCs. Cells were incubated with conditioned PBS, collected at days 1 ( $n = 6/\text{group}$ ) and 3 ( $n = 7/\text{group}$ ) in combination with  $25 \mu\text{M } H_2O_2$ . The survival rate was determined with an alamarBlue cell viability assay and normalized to alamarBlue baseline values. \* $p < 0.05$  and \*\* $p < 0.01$  compared to PBS supernatant using Student's t-test.